Muon Detection Based on a Hadronic Calorimeter

T. Ciodaro, on behalf of the ATLAS TDAQ collaboration.

***Abstract*—The ATLAS Tile hadronic calorimeter (TileCal) provides highly-segmented energy measurements of incoming particles. The information from TileCal's last segmentation layer can assist in muon tagging and it is being considered for a future upgrade of the level-one trigger to reject triggers due to radiation background effects in the barrel region. A muon receiver for the TileCal muon signals is being designed in order to interface with the ATLAS level-one trigger. This paper addresses the preliminary studies concerning the muon discrimination capability for the muon receiver. Monte Carlo simulations for single muons from the interaction point were used to study the effectiveness of hadronic calorimeter information for muon detection.**

ATL-DAQ-PROC-2010-050
21 November 2010

I. Introduction

THE Large Hadron Collider (LHC) is the largest and most complex machine ever built, located 100 m underground, in a 27 km long circular tunnel. LHC is designed to accelerate and collide bunches of protons near to the speed of light [1]. The collisions will happen at a very high rate (25 ns bunch-crossing), and at a center of mass energy up to 14 TeV, in order to increase the probability of observing interesting physics channels.

In order to detect and analyze the collision subproducts, particle detectors are placed around the collision points. Weighting 7,000 tons, with a length of 44 m and 22 m of diameter, ATLAS is the largest LHC detector [2]. ATLAS was designed to study a large range of physics topics such as supersymmetry, CP violation, dark matter, Higgs Boson, Standard model and beyond [2]. Figure 1 shows the ATLAS detector structure.

ATLAS is divided into two regions, according to the detector position along the LHC beam line: the barrel (long and extended), and the end-cap regions. Within these regions, there are three main subdetectors: the inner detectors, responsible for tracking charged particles, the calorimeters (comprising both electromagnetic and hadronic sections [3]), which are responsible for the energy measures, and the muon chambers, responsible for muons detection. The inner detectors and the muon chambers are also surrounded by an intensive magnetic field, solenoidal and toroidal, respectively, in order to bend particles coming from the collisions and to measure their momentum.

ATLAS produces around 1.5 MB of data per event [4], which results in an information flow of 60 TB/s. However, most of such data corresponds to well known physical processes and it is not interesting to the experiment. Thus, a sophisticated on-line filtering system (trigger) has been designed [4]. The trigger system filters out uninteresting events

T. Ciodaro is with the Signal Processing Laboratory - COPPE/Poli, Federal University of Rio de Janeiro, Brazil (e-mail: ciodaro@cern.ch).

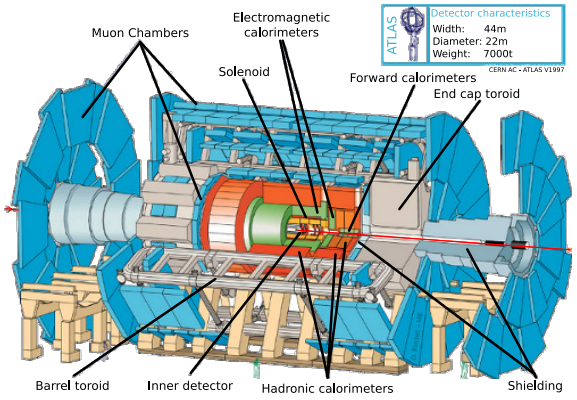

Figure 1. The ATLAS detector.

and records information from interesting processes, which are to be analyzed off-line (see Figure 2).

The on-line triggering is implemented into three cascaded levels. The first level (L1) is fully implemented in hardware and receives information from the muon chambers and the calorimeter with a coarse granularity. The L1 then selects regions of interest (RoI) to be used by the next level of triggers. The second and third levels are fully implemented in software. Unlike the L1, the second level (L2) operates with the full detector resolution, but usually within the RoI previously selected by the L1 (in order to reduce data access rates), and also it has access to the inner detectors information. The third level (Event Filter, EF) operates after the complete event is built (in the Event Builder), such that information from the entire detector can be used. The present work addresses the

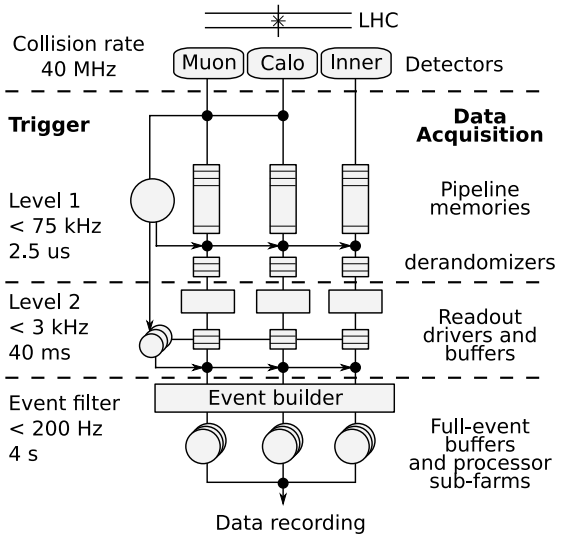

Figure 2. The ATLAS trigger schema.

first level (L1) trigger upgrade. This first level is responsible for the highest event rate reduction (to 75 kHz) in the shortest time (2.5 μ s).

Despite the fact that ATLAS has specific muon detectors, energy measurements from calorimeters can assist in muon identification at ATLAS. Though muons interact weakly with the calorimeters (producing signals with low signal-to-noise ratio), their energy measurements from calorimetry can improve the muon trigger performance. At L1, information from the ATLAS TileCal hadronic calorimeter can assist in rejecting fake triggers coming from non-collision particles [5].

This work studies the effectiveness of using calorimetry information to assist the muon spectrometer in L1 muon identification at the barrel region. As there are still no reliable simulations concerning the effects of fake triggers on the muon chambers, the present work addresses only the muon detection performance through the use of Monte Carlo simulations

The paper is organized as it follows. The next section briefly describes the current scenario of muon detection at ATLAS, the TileCal hadronic calorimeter and the Muon Spectrometer RPC detector. Section III refers to the muon receiver that is being under development for the ATLAS L1 trigger upgrade, which uses TileCal information for muon triggering. Section IV discusses the data used in this work and the tool used for muon tracking, while Section V presents the proposed matching for TileCal and muon chamber geometries. Finally, the simulation results are presented in Section VI and conclusions are derived in Section VII.

II. Muon Trigger

In the current trigger configuration, the muon chambers are responsible for muon detection, based on the estimation of the muon transverse momentum (p_T). Also, the correct p_T estimation is crucial for characterizing the physics channels of interest. In the level-one trigger (L1) only a rough estimation of the muon p_T is done. In higher levels, this information is better estimated through the use of ATLAS's full granularity.

In the second and third trigger levels, the track at the muon chambers is reconstructed and extrapolated to both the calorimeter and the inner detectors, reconstructing the full muon track from the interaction point. At this point, muon energy losses at the calorimeter can also be used to assist the track reconstruction.

A. The Muon Spectrometer

The Muon Spectrometer is responsible for triggering and measuring the muon transverse momentum, both in barrel and end-cap regions [6]. Monitored Drift Tubes (MDT) and Cathode Strip Chambers (CSCs) track the muons in a toroidal magnetic field for the barrel and for the end-cap regions, respectively. The L1 trigger is done through the Resistive Plate Chambers (RPCs), for the barrel, and Thin Gap Chambers (TGCs), for the end-cap.

RPC is divided into two sides, one for $\eta > 0$ and one for $\eta < 0$ [1]. From the trigger point of view, it is divided into 32

[1]The pseudorapidity η is defined as $\eta = -\ln\left(\tan\frac{\theta}{2}\right)$, where θ is the polar angle measured from the beam axis (z). The azimuthal angle ϕ is measured around the beam axis, with $\phi = 0$ pointing towards the center of LHC.

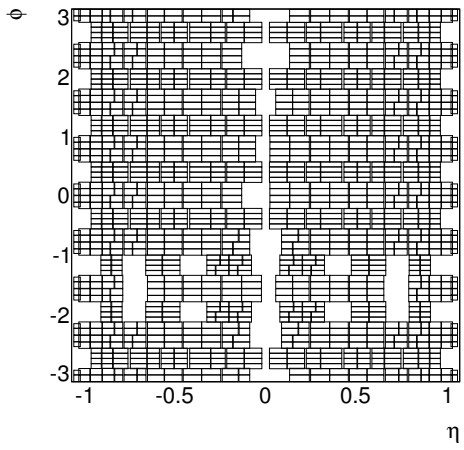

Figure 3. RPC RoI map.

trigger sectors per side. Each sector spans a region of 0.2×1.05 on the $\eta \times \phi$ plane, corresponding physically to a Sector Logic (SL) [7], while each SL is divided into several Regions of Interest (RoI) (See Figure 3). Further, RPC is formed of three distinct planes: the inner, outer and pivot planes (see Figure 4). Due to mechanical reasons, both Sector Logics and RoI's may present overlapped regions. Muons crossing these regions are handled in hardware by the RPC's readout system.

The RPC detector is able to trigger over 6 p_T thresholds (3 low-p_T and 3 high-p_T). When a muon candidate crossing the detector hits the pivot plane, the trigger algorithm searches for a confirmation hit on the inner and outer planes, applying the desired p_T thresholds simultaneously. Depending on the hitting characteristics, the muon candidate is classified and relevant information is sent to the Central Trigger Processor (CTP) for trigger decision [7].

During the detector commissioning, while the muon chambers were being assembled and calibrated, muons from cosmic rays [8] were triggered by calorimeter information. Specifically, TileCal signals were used by a special trigger configu-

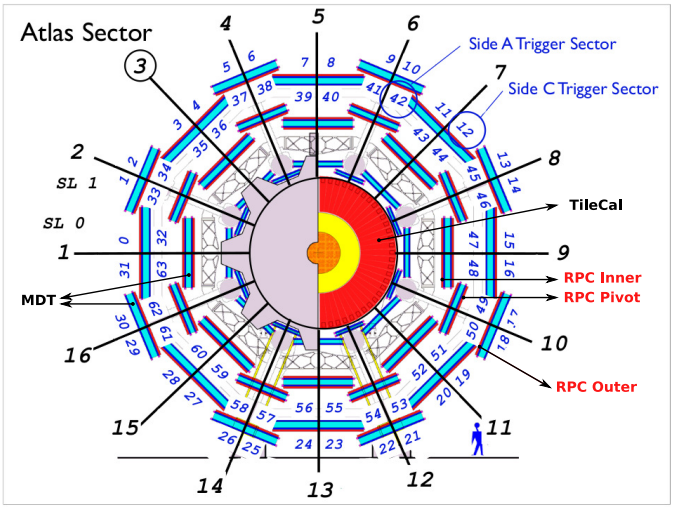

Figure 4. RPC detector schema.

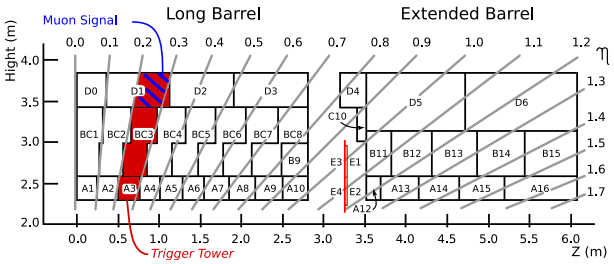

Figure 5. The TileCal cell geometry.

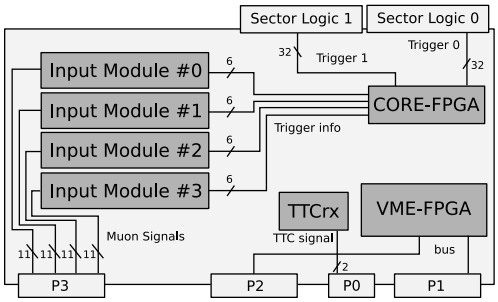

Figure 6. Receiver module scheme.

ration [9], and its muon discrimination capability was studied in detail.

B. Tile calorimeter

TileCal combines, side by side, steel plates as structure and absorber material, and plastic scintillating tiles as sampling material, grouped into cells of energy deposition [10] (see Figure 5). Incoming charged particles make the plastic tiles scintillate, while wave-length shifter fibers collect the produced light and transport it to a photomultiplier tube (PMT). The PMT is responsible for converting the luminosity information into an electrical signal, whose amplitude is directly proportional to the deposited energy. After pulse shaping, such electric signal is readout by the TileCal front-end electronics [11]. Each tile is connected to two different PMT's and readout channels. In this way, each cell has two independent readouts (labeled left and right), giving redundancy to the data acquisition.

The TileCal L1 interface card processes two readout signals [12]: a trigger tower (shaded region on Figure 5, spanning 0.1x0.1 on the $\eta \times \phi$ plane, which is used by the calorimeter trigger, and the muon signal, which is formed by the amplification of the last calorimeter layer (D cells) readout.

As the TileCal D cells are in the last calorimeter layer, they are less affected by hadronic activity and can be used for muon triggering. The final signals, though, have a very low signal-to-noise ratio, as muons interact weakly with matter.

C. Fake Triggers

The main source of fake triggers at the muon spectrometer is from non-collision particles, which are mainly due to the background radiation (commonly referred to as Cavern Background). Particularly thermal neutrons and low energy photons, bathing the detector during event pileup and afterward due to activation of materials in the detector, its support structure, and the cavern. The increase of particles flux at the muon spectrometer influences its parameters, such as the rate capability of chambers, the ageing of the detector components, the redundancy of the trigger instrumentation, the pattern recognition efficiency and others [13].

III. Muon Receiver

The TileCal muon receiver is being designed for the ATLAS L1 trigger upgrade. The main purpose of combining the TileCal D cell trigger and the RPC trigger is to reduce an unexpected high fake trigger rate due to cavern background. Nevertheless, the combined trigger cannot deteriorate significantly the muon detection at the L1 trigger.

The receiver is divided into two subsystems, one for each detector side (according to the η sign). Further, each subsystem hosts 32 receiver modules, each processing 44 D cell signals. In order to increase the signal-to-noise ratio, signals are routed to an input module, which analogically sums up the signals from the same TileCal D cell, before being digitized and readout [14].

The receiver module scheme can be seen on Figure 6. Each module receives signals from 24 TileCal D cells, spanning a region of 0.4 $\times$ 1.4 on the $\eta \times \phi$ plane. Even though the RPC detector covers up to 1.05 in η, the receiver current implementation is able to handle the entire TileCal range. Considering the RPC Sector Logic and TileCal module alignment in ϕ, a single receiver module is able to cover two SL.

After digitization, both signal detection and energy estimation are performed in order to discriminate from noise. Also, the incoming signal is assigned to the correct bunch-crossing in order to match with the RPC trigger. Finally, the CORE-FPGA collects information from all input modules, matches the TileCal muon trigger with the RPC geometry and transmits the final trigger information to the correct Sector Logic.

In the following sections, the L1 muon detection performance is evaluated for the combined trigger scenario.

IV. Monte Carlo Simulations

Within the ATLAS common software framework (Athena [15]) it is possible to access information from all other subdetectors, as well as information from all trigger levels and off-line analysis.

Simulations of single muons of 40 GeV/c momentum were used to study the performance of the combined trigger with respect to the RPC performance. For this, only muons detected by the off-line algorithms at RPC η range ($|\eta| < 1.05$) were analyzed. Then, each of these muons was matched to a RoI by means of a $\Delta R \equiv \sqrt{\Delta\eta^2 + \Delta\phi^2} < 0.5$, between the muon position at the Muon Spectrometer and the RoI coordinate.

The muon receiver performance was estimated from the results considering the simulation of the TileCal readout electronics, which have a signal-to-noise ratio greater than the TileCal D cells trigger. The estimated performance is, then, the best result that can be achieved by the detector.

A. Tracking

In order to correctly compare results, tracking information from the off-line reconstructed muon was used. Muon tracks from the Muon Spectrometer are matched to Inner Detector tracks, leading to an accurate estimation of the muon path inside the calorimeter. The cells on the muon path can be retrieved and TileCal D cells can be isolated. In this way, a muon detected by the off-line algorithms can be matched to a RPC RoI and a given TileCal D cell.

V. Geometry Matching

The trigger regions from TileCal and from RPC must be aligned. For TileCal, the base trigger region is the D cell, covering 0.2 $\times$ 0.1 in $\eta \times \phi$, while, for the RPC, the base trigger region is the RoI, which has different sizes. In this way, a straight mapping between D cells and RoI's is very complicated. Moreover, muons will bend because of the intensive magnetic field between TileCal and RPC, making it difficult to predict which RoI is hit from energy measurements at the TileCal D cell.

The proposed matching in this work is at Sector Logic (SL) level. Cells in TileCal are mapped onto a SL in the RPC. If any RoI is triggered in a given SL, a confirmation is required from the TileCal muon receiver, which should indicate if any cell corresponding to that SL was also triggered. Because of TileCal's geometry, the D cells at $\eta = 0.0$ (D0 cells) are split between A and C side. Whenever these cells are triggered, two SL are flagged, one at each side.

Because of mechanical reasons, RPC cannot fully cover the barrel region of $|\eta| < 1.05$ and, as a consequence, nearly 20 % of muons cannot be detected. Figure 7 shows the uncovered RPC regions corresponding to the magnet support structures (-2.3 $\leq \phi \leq$ -1.7 and -1.4 $\leq \phi \leq$ 0.9) and the Muon Spectrometer central crack around η = 0.0. An additional inefficiency arises from the magnetic ribs in small trigger sectors [16].

The TileCal extended barrel is not being used in the analysis presented in this work, as it has a small coverage over the RPC η range. Only half of one D cell at the extended barrel is below $|\eta| < 1.05$ and its removal from the combined trigger can simplify the required hardware.

VI. Simulation Results

The combined trigger performance is measured with respect to the RPC efficiency. As TileCal is not meant to be used as a muon detector, a combined trigger between TileCal and RPC is likely to deteriorate the muon identification efficiency at the L1 trigger, but the fake muon rate can be reduced.

The results were derived according to the geometry matching described in Section V. The information from off-line track extrapolation was used to correctly match a RoI and a D cell. Although this information is not available at the L1 trigger, it was used in this work as a benchmark.

Figure 8 shows the muon detection performance with respect to the RPC efficiency, as a function of the energy threshold used at the TileCal D cells. Only muons that cross the TileCal long barrel ($|\eta| < 0.7$) are considered, as the TileCal

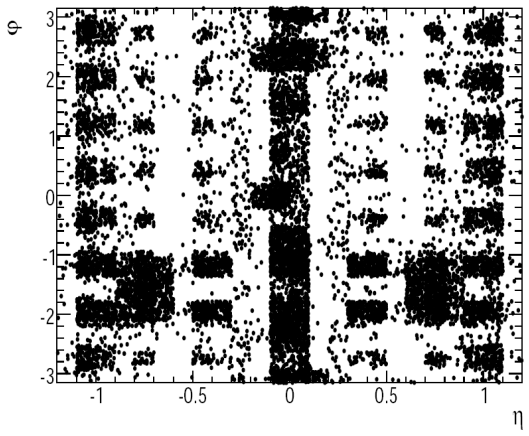

Figure 7. RPC geometrical acceptance is approximately 80 %, extracted from [16].

crack region and extended barrels ($|\eta| > 0.7$) are triggered by RPC only (with no confirmation trigger from TileCal). It can be seen that the results for the benchmarking approaches unity when the energy threshold is raised to the simulated noise level at the TileCal readout electronics ($3\sigma \approx 75\ MeV$). The comparison with the results for the SL match shows that this geometry matching leads to almost a 6.5 % inefficiency with respect to the RPC performance. This is due to muons that hit TileCal and RPC in different ϕ positions, failing the SL matching, and it can arise from: muons that were bent in ϕ due to the magnetic field at the Inner Detector, mismatches because of how overlapped Sector Logics are treated at the RPC electronics, and muons that interacts with the detector and might have their trajectory deviated in ϕ.

Figure 9 shows the muon detection performance with respect to RPC's performance as a function of η. The energy thresholds for the TileCal D cells were set to 200 MeV, which is around the end of the performance plateau seen on Figure 8. It can be seen that the combined performance is more or less flat along η, however with a small drop of performance around

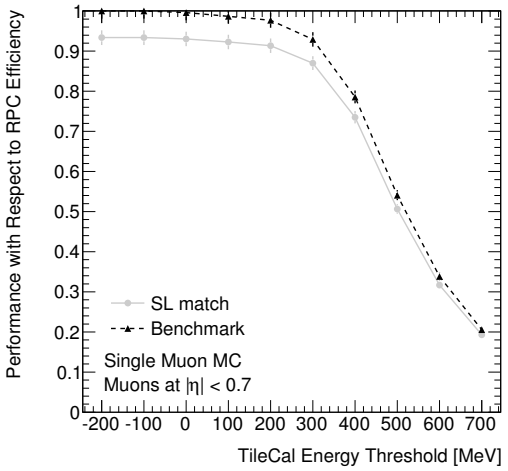

Figure 8. Performance for the combined trigger with respect to RPC's efficiency.

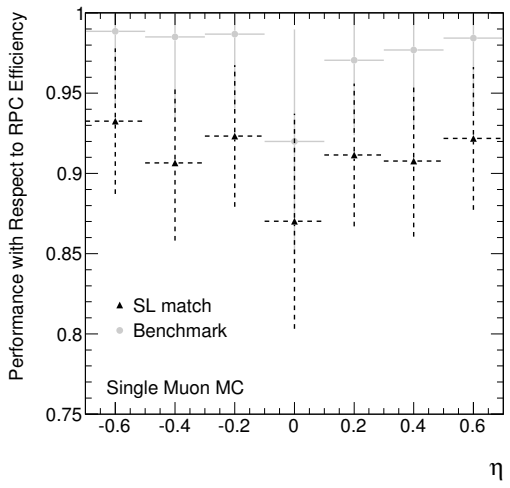

Figure 9. Performance for the combined trigger with respect to RPC's performance.

$\eta \approx 0$. This can be understood because the energy distribution for the D cell at $\eta \approx 0$ is closer to the threshold cut than for the other cells at different η.

VII. Conclusions

Monte Carlo simulations for single muons with 40 GeV/c momentum originating from the interaction point were used to evaluate the combined performance of TileCal and RPC triggers for the first level on-line filtering system operation.

The geometry matching between TileCal D cells and RPC RoI's was evaluated. Matching from off-line track extrapolations was used as benchmark, though this information is not available at the ATLAS L1 trigger. The proposed matching, at the Sector Logic level, reduced the efficiency by approximately 6.5 %. The performance with respect to the RPC efficiency, as a function of η, showed that the energy threshold applied is not optimized for each D cell and a fine tuning is still needed.

Finally, the results showed that the use of TileCal to assist the RPC detector in muon tagging do not deteriorate significantly the L1 performance. A trade-off between muon detection and cavern background rejection must still be evaluated, in order to confirm the feasibility of the combined trigger, as well as the performance estimation with respect to the muon signals from the D cells themselves.

Acknowledgment

We are thankful for the support that has been provided to this work by CNPq, FINEP, RENAFAE and FAPERJ (Brazil), CERN and the Europe Union (through the HELEN program). We would also like to thank our colleagues from the ATLAS TileCal and TDAq collaborations for all the support and interesting discussions concerning this work.

References

[1] L. Evans et al., "LHC machine," *Journal of Instrumentation*, vol. 1, no. 2008 JINST 3 S08001, August 2008.

[2] G. Aad et al., "The ATLAS experiment at the CERN large hadron collider," *Journal of Instrumentation*, vol. 1, no. 2008 JINST 3 S08003, August 2008.

[3] R. Wigmans, *Calorimetry: Energy Measurement in Particle Physics*, ser. International series of monographs on physics. Oxford: Clarendon Press, 2000.

[4] K. Kordas et al., "The ATLAS Data Acquisition and Trigger: concept, design and status," *Nuclear Physics B - Proceedings Supplements*, vol. 172, pp. 178 – 182, 2007.

[5] ATLAS/Tile Calorimeter Collaboration, "Tile Calorimeter Technical Design Report," 1996, CERN/LHCC 96–42.

[6] R. Nicolaidou and B. Resende, "Muon track reconstruction in the atlas experiment," vol. 1. Conference Record for IEEE Nuclear Science Symposium, 2008, pp. 864–866.

[7] F. Anulli et al., "The Level-1 Trigger Muon Barrel System of the ATLAS experiment at CERN," *Journal of Instrumentation*, p. P04010. 37 p, Jan 2009.

[8] T. K. Gaisser, *Cosmic rays and particle physics*. Cambridge: Cambridge Univ. Press, 1990.

[9] B. Ferreira et al., "Cosmic Ray Triggering Using Muon Signal Detected by the Hadronic Calorimeter of ATLAS," *The Journal of High Energy Physics*, vol. ACAT, pp. 1–8, 2007.

[10] F. Ariztizabal et al., "Construction and performance of an iron-scintillator hadron calorimeter with longitudinal tile configuration," *Nuclear Instruments and Methods in Physics Research Section A*, vol. 349, pp. 384 – 397, 1994.

[11] K. Anderson et al., "Design of the front-end analog electronics for the ATLAS tile calorimeter," *Nuclear Instruments and Methods in Physics Research A*, vol. 551, pp. 469–476, October 2005.

[12] A. Cerqueira et al., "Analog System for Building the First-Level Triggering Signal Provided By the Hadronic Calorimeter of ATLAS Detector," *Nuclear Instruments and Methods in Physics Research Section A*, vol. 570, pp. 117–125, 2007.

[13] S. Baranov, M. Bosman, I. Dawson, V. Hedberg, A. Nisati, and M. Shupe, "Estimation of radiation background, impact on detectors, activation and shielding optimization in atlas," CERN, Geneva, Tech. Rep. CERN-ATL-GEN-2005-001, Jan 2005.

[14] T. Ciodaro et al, "A Receiver System for the TileCal Muon Signals," vol. 1. Conference Record for IEEE Nuclear Science Symposium, 2009, pp. 1–8.

[15] K. Cranmer, K, "The ATLAS Analysis Architecture," vol. 177. Nuclear Physics B - Proceedings Supplements, 2007, pp. 126–130.

[16] G. Aad et al, *Expected performance of the ATLAS experiment: detector, trigger and physics*. Geneva: CERN, 2009.